



Thermal behavior of entacapone, a catechol-*O*-methyltransferase inhibitor used in Parkinson's disease

Titus Vlase¹ · Paul Albu^{1,2} · Adriana Ledeti³ · Denisa Cercioban³ · Mădălina Mateescu¹ · Codruța Moșoiu¹ · Gabriela Vlase¹ 

Received: 30 November 2017 / Accepted: 20 February 2018 / Published online: 6 March 2018
© Akadémiai Kiadó, Budapest, Hungary 2018

Abstract

Entacapone, a selective and reversible inhibitor of catechol-*O*-methyltransferase, is used in the treatment of Parkinson's disease in combination with levodopa/carbidopa to treat the symptoms of end-of-dose “wearing-off” effect. Considering that new formulations are researched constantly, proper knowledge of the active pharmaceutical ingredients is crucial in the preformulation stages. Kinetic analysis was performed using three methods: one integral—Flynn–Wall–Ozawa method, one differential—Friedman method, and modified nonparametric kinetics method (NPK). The thermoanalytical curves were registered at five different heating rates: $\beta = 5, 7, 10, 12,$ and $15 \text{ }^\circ\text{C min}^{-1}$. Analysis was conducted in the dynamic air atmosphere to highlight potential thermooxidative processes. This paper deals with the investigation of solid-state stability and compatibility of binary mixture of entacapone with various pharmaceutical excipients by two instrumental techniques, such as universal attenuated total reflection Fourier transform infrared and thermal analysis (TG/DTG/HF). The excipients used in the mixture were: mannitol, silicon dioxide, talc, sorbitol, magnesium stearate, and povidone.

Keywords Entacapone · Compatibility study · Excipient · FTIR · Thermal analysis · Kinetic study

Introduction

Parkinson's disease, the second most common neurodegenerative disorder that affects millions of people all over the world, is known to be a condition in which the patients develop gradually over time motor, behavioral, and cognitive symptoms. The main affected structures are the dopaminergic neurons from the basal ganglia which lead to decreased dopamine levels in the central nervous system (CNS) [1, 2].

The main treatment is based on levodopa, a dopamine precursor that crosses over the blood–brain barrier and gets metabolised into the active substance. In order to avoid increasing the dose and administration frequency of levodopa, which in turn would elevate the risk of side effects, an adjunct is added to the treatment, such as a compound from the catechol-*O*-methyltransferase (COMT) inhibitors class, entacapone among them [3, 4].

Entacapone ((*E*)-2-cyano-*N,N*-diethyl-3-(3,4-dihydroxy-5-nitrophenyl)acrylamide) is a member of the class of nitrocatechols with a high lipophilicity [5], and also it is a reversible, peripheral, selective COMT inhibitor, which is an enzyme involved in the metabolism of levodopa [6–9]. By inhibiting the action of the enzyme, levodopa is not decomposed in the peripheral area and higher concentrations can reach the CNS to be converted into dopamine [10, 11]. When administered in association with levodopa, entacapone is able to prolong its half-life by almost 2.4 h, allowing the administration of levodopa in patients with advanced stages of the disease in a smaller dose, with a decreased frequency and assuring the lack of the wearing-off effect [4, 12, 13].

✉ Gabriela Vlase
gabriela.vlase@e-uvv.ro

¹ Research Centre for Thermal Analysis in Environmental Problems, West University of Timisoara, Pestalozzi Street 16, 300115 Timisoara, Romania

² Department of Pharmacy, Faculty of Medicine, Pharmacy and Dentistry, Vasile Goldiș West University of Arad, L. Rebreanu Street 86, 310414 Arad, Romania

³ Faculty of Pharmacy, University of Medicine and Pharmacy “Victor Babeș”, Eftimie Murgu Square 2, 300041 Timisoara, Romania

Considering the fact that the main action mechanism involves increasing levodopa's bioavailability, it is only natural that entacapone's side effects are related to increased dopaminergic stimulation [14]. These include hyperkinesia or dyskinesia, nausea, vomiting, diarrhea, or even hallucinations, all possibly reduced by adjusting the dose of levodopa [6, 7].

The absorption of entacapone is complete and fast, but it has a limited bioavailability, this fact due to the hepatic first-pass metabolism [5]. Nitro group presence at the ortho position to the hydroxyl group is essential for entacapone potency and ability to inhibit COMT [15].

Entacapone can be found as a single active substance as a tablet formulation or in association with levodopa and a dopa-decarboxylase inhibitor, such as carbidopa [1, 16]. The use of this combination allows an increased flexibility regarding the necessary dose while providing a higher treatment adherence by avoiding the need to administer multiple pills [17].

Until this moment ENT was study taking in consideration the different mode of administration, it was found in the literature as being delivered in the form of self-microemulsifying drug delivery systems [18], microspheres [19] microcapsules [4], without study regarding on thermal behavior.

By analyzing these facts along with the knowledge that the prevalence of Parkinson's disease is more concerning as years go by, we consider it necessary to provide a complete physicochemical profile of entacapone in order to assure that in the ongoing drug design processes involving this substance, all fundamental information imperative in the preformulation stages is known.

The kinetic parameters of ENT were studied using TG/DTG curves with Friedman (Fd), Flynn–Wall–Ozawa (FWO), Kissinger–Akahira–Sunose (KAS), and Li–Tang (LT) methods [20].

Regarding its physicochemical properties, it is known that entacapone (Fig. 1) is a yellow or green–yellow powder, with a molecular weight of 305.29 g mol⁻¹ and a melting point of 162–163 °C, poorly soluble in water (79 mg L⁻¹), soluble in acetone and anhydrous ethanol [21–24].

The 3,4-dihydroxy-5-nitrobenzylidene derivative is a weak acid that has a pKa value of 4.5 whose water solubility varies significantly with pH values. At acidic pH values, entacapone's solubility is quite low (12.4 µg mL⁻¹ at pH 3.0) and it increases as pH increases to more basic pH values (1750 µg mL⁻¹ at pH 7.5) [25]. This fact may be considered problematic because the low pH levels of gastric fluids may be unfavorable to the substance's solubility and therefore its bioavailability [17]. As for its dissolution rate, the values are much higher for increased pH values than for acidic ones, property explained by the

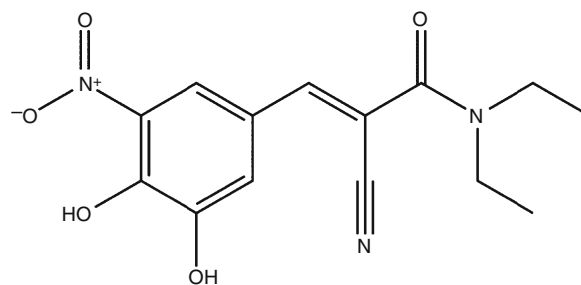


Fig. 1 Chemical structure of entacapone

completely ionized form in which entacapone is found at pH 7.5 [25].

Because of these properties, alternative administration pathways are researched and even possible derivatives are being taken under advisement. In order to successfully obtain new pharmaceutical formulations, further analysis regarding the behavior of entacapone under various thermal conditions is required.

Materials and methods

The present study was performed in the dynamic air atmosphere to highlight potential thermooxidative processes for pure active substance and even for binary mixtures.

The active substance, entacapone (Enta) was purchased from Sigma (SML0654). The structure of the active substance is presented in Fig. 1. The excipients used for the compatibility study with active substance are: mannitol (Merck Germany), silicon dioxide (SiO₂) (Aerosil 200 Evonik Degussa, Germany), talc (Luzenac Pharma, Italy), sorbitol (Sorb) (Sigma, Germany), magnesium stearate (MgSt) (Union Derivan, Spain), hydroxyethyl cellulose (HEC) (Merck Germany), and povidone (PVP) (Sigma).

The studies were performed on the pure substance and on binary mixtures of active agent and excipients (1:1, w/w). The mixtures were prepared manually at room temperature and then stored in a refrigerator until analysis. For the study of interaction by spectroscopic techniques, binary mixtures (active substance: excipient) were kept for 6 weeks without humidity and light at room temperature.

FTIR spectra were collected in the 4000–650 cm⁻¹ spectral range, with a resolution of 1 cm⁻¹ and 16 co-added scans using a PerkinElmer SPECTRUM 100 spectrometer with universal attenuated total reflection Fourier transform infrared spectra (UATR-FTIR).

The thermal behavior for all of the samples was recorded in the air atmosphere with a flow rate of 100 mL min⁻¹, using five different heating rates: $\beta = 5, 7, 10, 12, \text{ and } 15 \text{ } ^\circ\text{C min}^{-1}$ until 500 °C on a TG/DTA

Diamond thermobalance produced by PerkinElmer in aluminum crucible.

Data were collected via PerkinElmer Pyris software. As kinetic methods, integral methods (Flynn–Wall–Ozawa) and one differential method (Friedman) were used. This analysis was completed by using the nonparametric kinetics method (NPK).

Results and discussions

Thermogravimetric analysis

Entacapone shows the TG curve obtained at a heating rate of $10\text{ }^{\circ}\text{C min}^{-1}$ to $500\text{ }^{\circ}\text{C}$ in air at a flow rate of 100 mL min^{-1} , a decomposition process with a loss of 32.88% in the range of $195\text{--}290\text{ }^{\circ}\text{C}$. The process can be also highlighted by the DTG and heat flow curves. The process of mass loss is an exothermic process with a maximum at $247\text{ }^{\circ}\text{C}$ and a ΔH of -539 J g^{-1} with a maximum at $256\text{ }^{\circ}\text{C}$. The decomposition process is accompanied by a melting process at $164\text{ }^{\circ}\text{C}$. This process is continued by a mass loss in the range of $290\text{--}347\text{ }^{\circ}\text{C}$, a 5.68% mass loss that is observed on the heat flow curve with a weak exothermic effect. The active substance exhibits relatively high thermal stability (Fig. 2).

From the analysis of the thermoanalytic curves in the interval $195\text{--}347\text{ }^{\circ}\text{C}$, there are two degradation processes that can not be separated very well. In this temperature range, it is possible to simultaneously lose the *T*-butylamide molecule and the nitrite molecule.

The calculated mass loss is 38.70%, and the experimental mass loss is 38.56% [20]. The two stages of decomposition obtained in the air atmosphere cannot be

separated, so we can say that there are two parallel decomposition processes. Therefore, the study will be complemented with kinetic analysis by the NPK method, which can highlight the complex decomposition stages. The decomposition of the active substance in this temperature range is a complex decomposition.

FTIR spectra

In this study the FTIR spectra of the active substance were drawn up before and after thermal treatment at $350\text{ }^{\circ}\text{C}$ and are comparatively presented in Fig. 3.

A temperature of $350\text{ }^{\circ}\text{C}$ was chosen because at this temperature, the active substance lost almost 38% of the sample mass. From the FTIR spectra made on the degraded active substance at $350\text{ }^{\circ}\text{C}$, it is possible to emphasize the vibrations of the bonds that disappear from the spectrum of the initial substance after the thermal treatment.

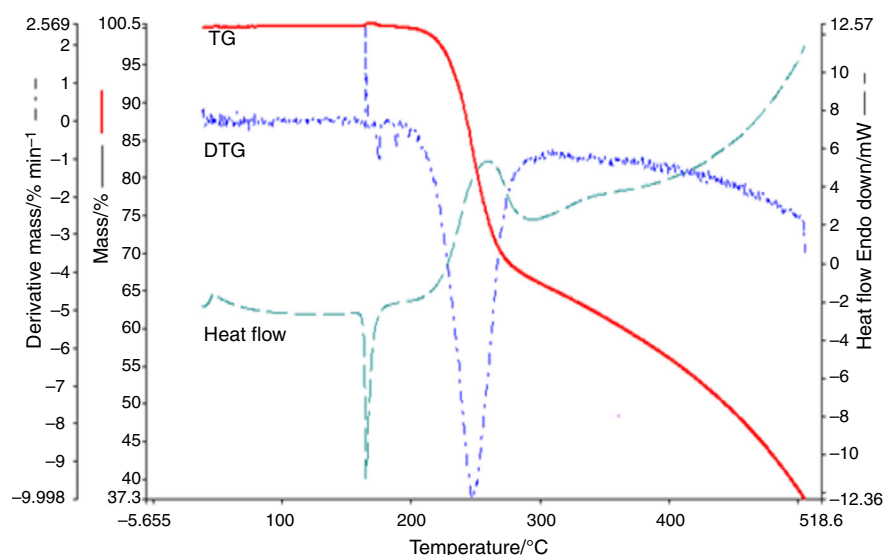
From the FTIR spectra of the active substance treated at $350\text{ }^{\circ}\text{C}$, disappear the peaks in spectral range: $2976\text{--}2880$, $1525\text{--}1480$, $1295\text{--}1275$, $820\text{--}775$, and $720\text{--}665\text{ cm}^{-1}$ which argues the losses of *T*-butylamide molecule.

The disappearance of the strips in the $3360\text{--}3220$ and $1625\text{--}1610\text{ cm}^{-1}$ regions can be attributed to the loss of the aromatic nitrite group.

Kinetic study

The kinetic parameters of the process of thermal degradation of Ent were determined from data collected at five different heating rates: $\beta = 5, 7, 10, 12,$ and $15\text{ }^{\circ}\text{C min}^{-1}$ using open aluminum crucible in a TG/DTA Diamond thermobalance PerkinElmer in air atmosphere (Lindegas, 5.0) with a flow rate of 100 mL min^{-1} .

Fig. 2 Thermoanalytical curves obtained with a heating rate of $10\text{ }^{\circ}\text{C min}^{-1}$ – $500\text{ }^{\circ}\text{C}$ in air atmosphere



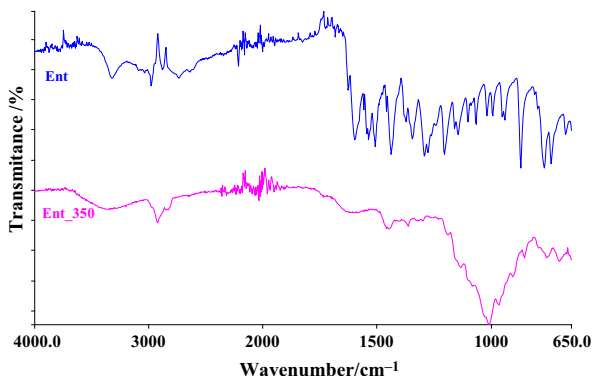


Fig. 3 FTIR spectra of the active substance initially and thermally treated at 350 °C

Starting from the generally accepted axiom that the reaction rate can be expressed as a product of two separate functions, i.e.,

$$d\alpha/dt = k(T) \cdot f(\alpha) \quad (1)$$

where t is time, T is temperature, and $f(\alpha)$ is the reaction model.

The Friedman's differential–isoconversional method (FR) [26]

For a single-step process and a heating rate β , Eq. (1) becomes:

$$(\beta \cdot d\alpha/dT)_\alpha = k(T) \cdot f(\alpha) \quad (2)$$

where β is the heating rate, A and E —the preexponential factor, respectively, the activation energy $\beta \cdot (d\alpha/dT)$ is the direct available from DTG data, and $f(\alpha)$ is the conversion function.

Because for solving Eq. (2) so many strategies were suggested, with additional axioms and approximations, we

consider that a believable kinetic study requires at least three different methods.

By linearization of Eq. (2) in the form

$$[\ln(\beta \cdot d\alpha/dT)]_\alpha = \ln[A \cdot f(\alpha)]_\alpha - E/RT, \quad (3)$$

the value of E will be determinate.

At a certain conversion, the slope of the straight line of $\ln[\beta(d\alpha/dT)]$ versus $1/T$ gives the activation energy (see Fig. 4). Because the conversion function $f(\alpha)$ is not explicit, the Friedman's method is considered a “model free” method.

The integral method by Flynn–Wall and Ozawa (FWO) [27, 28]

By integration of Eq. (3), it becomes:

$$[\ln \beta = \ln A/[R \cdot g(\alpha)] - 5.331 - 1.052 \cdot E/RT,] \quad (4)$$

where $[g(\alpha) = \int \frac{d\alpha}{f(\alpha)}]$ is the integral conversion function. By plotting of the left member of Eq. (4) versus $1/T$, the value of the activation energy will be obtained from the line slope (see Fig. 4).

Variations in E versus α exceed 10%, and these variations are non-monotonous. Therefore, a mean value of the activation energy is reasonable only for comparison (see Table 1).

The nonparametric kinetic method

The NPK method, elaborated by Nomen and Sempere [29, 30] for processing of isothermal DSC data, was subsequently modified and largely applied in non-isothermal kinetic analysis [31–33].

The reaction rates, $r = d\alpha/dt$, obtained at different heating rates, were represented in a 3-D coordinate system (r, T, α) and interpolated by a proper algorithm so that a

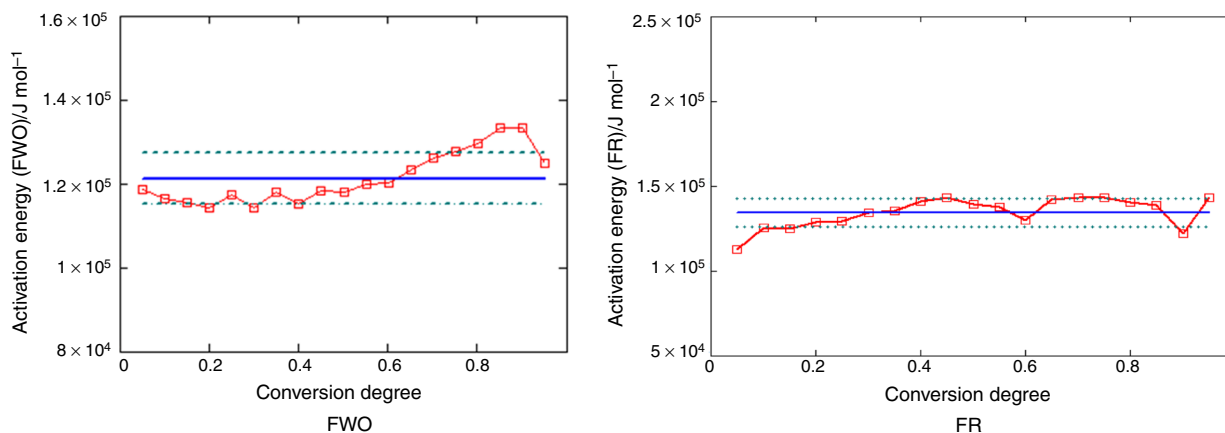


Fig. 4 Variation in activation energy with degree of conversion for FR, respectively, FWO methods

Table 1 Comparative activation energy obtained by FR, FWO, and modified NPK methods

$[\bar{E}_{FR}]/\text{kJ mol}^{-1}$	$[\bar{E}_{FWO}]/\text{kJ mol}^{-1}$	$[\bar{E}_{NPK}]/\text{kJ mol}^{-1}$
121 ± 6	134 ± 8	122 ± 15

continuous reaction rate surface was obtained (Fig. 5a). Based on the assumption that the reaction rate can be expressed as a product of two independent functions, $f(T)$ and $g(\alpha)$, the obtained surface was organized as an $i \times j$ matrix, where the rows correspond to different degrees of conversion and the columns correspond to different temperatures.

$$[\mathbf{M} = \{m_{ij}\} = \{f(T_i) \cdot g(\alpha_j)\}] \quad (5)$$

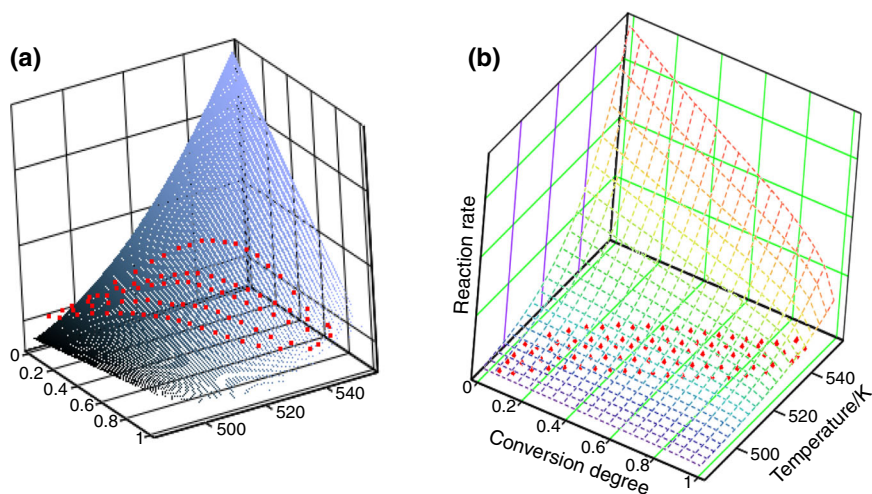
Using the singular value decomposition (SVD) algorithm [34], the matrix was decomposed according to:

$$[\mathbf{M} = \mathbf{U}(\text{diag} \cdot \mathbf{s})\mathbf{V}^T] \quad (6)$$

A vector \mathbf{u}_1 (the first column of \mathbf{U}) was analyzed in respect of dependence on the conversion degree, according to the equation suggested by Šestak and Berggren [35]:

$$[g(\alpha) = \alpha^m(1 - \alpha)^n], \quad (7)$$

where α^m describes the influence of physical phenomenon related to the presence of reaction product and $(1 - \alpha)^n$ describes the chemical phenomenon which implies the remaining reactant $(1 - \alpha)$.

Fig. 5 Reaction rate surface (a interpolated; b recalculated with data from Table 2) and experimental points**Table 2** Kinetic parameters obtained from NPK

Process	$\lambda/\%$	A/s^{-1}	$E/\text{kJ mol}^{-1}$	n	m	Corr. coef.	$[\bar{E}]/\text{kJ mol}^{-1}$
Main	88.0	3.14×10^{12}	120 ± 14	1/3	–	0.996	122 ± 15
Secondary 1	6.6	2.24×10^{14}	133 ± 0.3	2	–	0.998	
Secondary 2	5.4	3.59×10^{12}	134 ± 1	1	–	0.993	

A similar vector, \mathbf{v}_1 (corresponding to matrix \mathbf{V}) was checked for an Arrhenius-type temperature dependence.

If the degradation process is a complex one, for example, with two simultaneous reactions having the rate r_1 and r_2 , then the observed reaction rate will be:

$$[r = r_1 + r_2] \quad (8)$$

and consequently

$$[\mathbf{M} = \mathbf{M}_1 + \mathbf{M}_2 = \mathbf{U}_1(\text{diag} \cdot \mathbf{s}_1)\mathbf{V}_1^T + \mathbf{U}_2(\text{diag} \cdot \mathbf{s}_2)\mathbf{V}_2^T] \quad (9)$$

The contribution of each step to the observed process will be expressed by the explained variance λ , so that $\lambda_1 + \lambda_2 = 100\%$.

By applying this data processing strategy, a discrimination between two or more simultaneous processes is possible. Also the SVD algorithm allows a “natural” separation of the influences of the temperature, respectively, conversion degree.

The data obtained by applying the modified NPK method on TG/DTG data processing are systematized in Table 2. The recalculated reaction surface with data from Table 2 is presented in Fig. 5b.

Thermal decomposition into the air atmosphere of Ent is a complex process that tends to take place in several stages with about the same share. This complex process was also revealed by the NPK kinetic method. One predominant process is observed and two other parallel processes with a

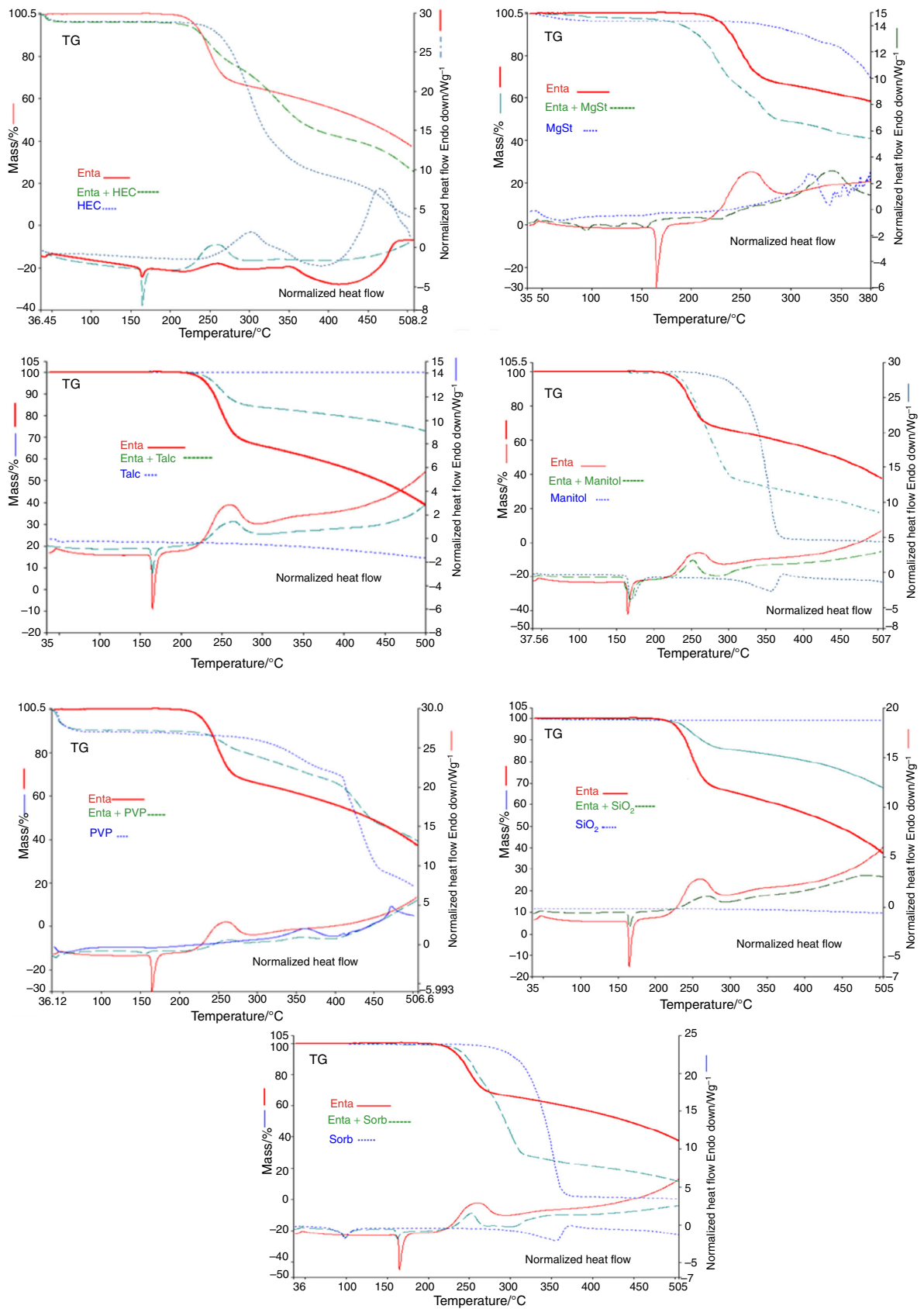


Fig. 6 Thermoanalytical curves obtained for binary mixtures (Ent + excipients)

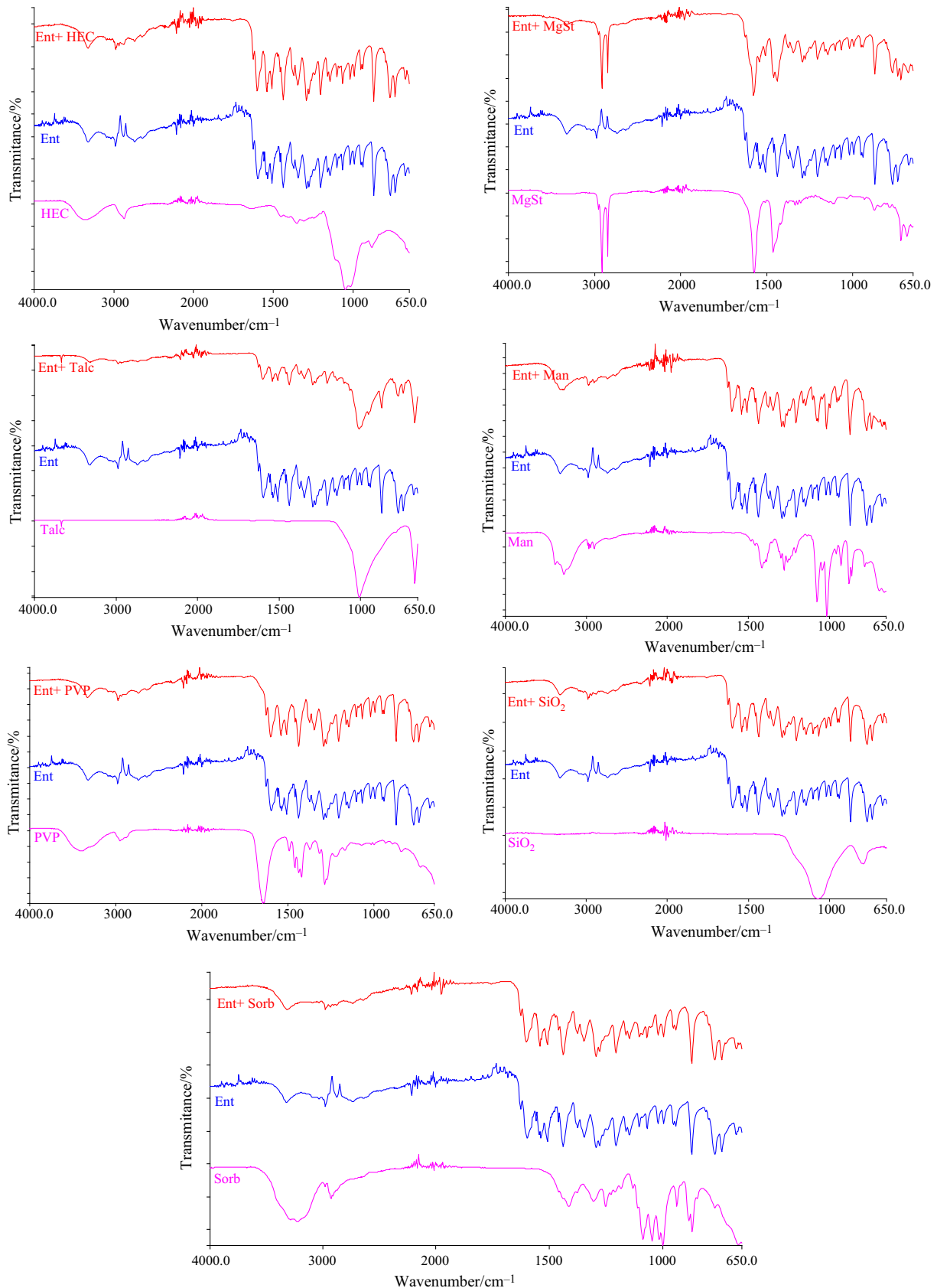
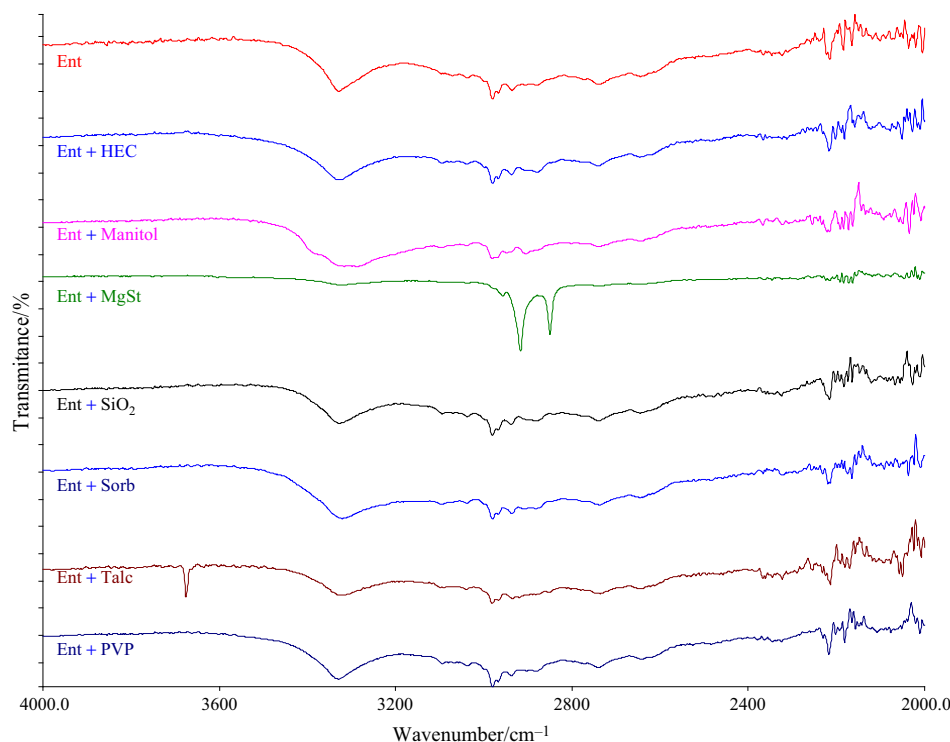


Fig. 7 FTIR spectra of Ent/binary mixtures/excipient

Fig. 8 UATR–FTIR of binary mixtures in 4000–2000 cm^{-1} spectral regions



near share, with E_a close to E_a (FWO) occurring at conversions greater than 0.7. This observation explains the impossibility of separating them on the TG and DTG curves. All processes identified by NPK are chemical processes $n \pm 0$, and physical processes $m = 0$ have not been revealed.

The kinetic study achieved by the three methods: differential–isoconversional (FR), integral–isoconversional (FWO), and nonparametric method (NPK); results have been achieved in good correlation (Table 1).

Thermal analysis of binary mixture (Fig. 6)

The TG curve obtained with the Enta + HEC mixture is a combination of the decomposition curves obtained with the individual components.

On the heat flow curve of the mixture is observed the thermal behavior of the active substance up to 280 °C. Above this temperature, we cannot identify the implication of the excipient in the mixture, which leads us to the conclusion that there are thermally induced interactions.

The same can be said about the Ent + Manitol and Ent + Sorb mixtures when over 280 °C thermal behavior indicates a thermally induced interaction.

Analyzing the thermoanalytic curves obtained in the case of Ent + SiO_2 and Ent + talc mixtures, we can say that the excipients are inert in these pharmaceutical mixtures. No thermally induced interactions occur. The TG and

heat flow (HF) curves of mixtures are combinations of curves of individual components.

The HF curve obtained in case of Ent + MgSt mixture reveals a completely different behavior compared to that of the individual components. In the case of MgSt, the HF curve shows three endothermic peaks at temperatures lower than the melting temperature of the pure active substance. The HF curve of the Ent + PVP mixture shows the peak of melting entacapone at a lower 20 °C temperature, but this shift can be explained by the fact that the active substance is mixed.

We can say that at temperatures below 200 °C, interactions occur between Ent and MgSt. Polividona (PVP) does not exhibit thermally induced interactions with Ent.

FTIR study of binary mixture

To realize the compatibility studies between entacapone and excipients by spectroscopic techniques, binary mixtures (active substance: excipient) were maintained for 6 weeks in the absence of light and humidity at room temperature.

The FTIR spectra obtained in binary mixtures were compared with the FTIR spectra of the individual components in order to be able to highlight possible interactions between the components.

The FTIR spectra of the binary mixtures are shown in Figs. 7 and 8.

Entacapone {(2*E*)-2-Cyano-3-(3,4-dihydroxy-5-nitrophenyl)-*N,N*-diethylacrylamide} is a compound with alkyl groups, hydroxy- and amino-group aromatic and C≡N bonds. Interactions with the functional groups of the excipients may take place in these groups. Analyzing the FTIR results, several conclusions can be drawn.

The band [36] in the spectral region 3450–3300 cm⁻¹ characteristic for alchil group, hidroxy or amino present in case of active substance is found in most binary mixtures, and it is more intense in case of excipients with O–H groups in the molecule.

A clear change appears to occur in the spectrum of the binary mixture Ent + MgSt in the 3450–3300 cm⁻¹ region (see Fig. 6); the bands are drastically attenuated. The disappearance of band 2980 and 2880 cm⁻¹ characteristic of entacapone is also observed. In the FTIR spectra of the mixture, the bands in this region characterized by MgSt are strongly visible.

In the case of the other mixtures, no clear differences are observed, both the active substance bands and the excipient bands being visible. We can say that after the spectroscopic technique, interactions at room temperature can only be observed in the Ent + MgSt mixture.

The results obtained in case of binary mixtures by thermoanalytic techniques and spectroscopic techniques were the same:

- are present interactions at room temperature only for the Ent + MgSt mixture;
- There are no interactions in case of Ent + SiO₂, Ent + Talc and Ent + PVP mixtures,
- Thermally induced high-temperature interactions (280 °C) occur in case of Ent + Manitol, Ent + Sorb, and Ent + HEC mixtures.

Conclusions

In this study, the investigation regarding the thermal stability of entacapone active substance and the mixture of this substance with seven excipients was discussed.

The investigations were performed in solid state, using FTIR spectroscopy, thermal analysis and kinetic study of active substance.

The thermogravimetric study conducted in air atmosphere highlighted the thermal decomposition that was in good correlation with the mass losses attributed. In the air atmosphere was found the presence of a complex decomposition process, which was also argued by the kinetic study performed by the NPK method.

The kinetic study is achieved by the three methods: differential isoconversional (FR), integral isoconversional (FWO), and nonparametric method (NPK); results have

been achieved in very good correlation. The NPK kinetic method highlights a predominant process and two other processes parallel to a close share. All processes identified by NPK are chemical processes $n \neq 0$, and no physical processes have been identified $m = 0$.

Active substance–excipient compatibility studies performed using thermoanalytic techniques and spectroscopic techniques have led to the same results.

This preformulation study can be a starting tool for the selection of adequate excipients in new solid dosage forms that contain entacapone as active substance.

Acknowledgements This work, for Gabriela Vlase, Adriana Ledeti, and Denisa Circioban, was supported by the PN-II-RU-TE-2014-4-0515.

References

1. Tarazi FI, Schetz JA (eds). Neurological and psychiatric disorders. United States. 2005: ISBN 978-1-59259-856-4; <https://doi.org/10.1385/1592598560>.
2. Potturi PK, Sudhakar Y. Formulation and in vitro/in vivo evaluation of controlled release Entacapone trilayer matrix tablets by geomatrix. *Int J Drug Deliv.* 2015;7:155–66.
3. Paci C, Sanguigni S, Carboni T, Gobbato R, Curatola L. The use of entacapone in patients with advanced Parkinson's disease: 2 years' experience. *Neurol Sci.* 2003;24(3):197–8.
4. Baek JS, Choo CC, Qian C, Tan NS, Shen Z, Loo SCJ. Multi-drug-loaded microcapsules with controlled release for management of Parkinson's disease. *Small.* 2016;12:3712–22.
5. Grünig D, Felser A, Bouitbir J, Krähenbühl S. The catechol-*O*-methyltransferase inhibitors tolcapone and entacapone uncouple and inhibit the mitochondrial respiratory chain in HepaRG cells. *Toxicol Vitro.* 2017;42:337–47.
6. Keranen T, Gordin A, Karlsson M, Korpela K, Pentikainen PJ, Rita H, Schultz E, Seppala L, Wikberg T. Inhibition of soluble catechol-*O*-methyltransferase and single-dose pharmacokinetics after oral and intravenous administration of entacapone. *Eur J Clin Pharmacol.* 1994;46(2):151–7.
7. Piccini P, Brooks DJ, Korpela K, Pavese N, Karlsson M, Gordin A. The catechol-*O*-methyltransferase (COMT) inhibitor entacapone enhances the pharmacokinetic and clinical response to Sinemet CR in Parkinson's disease. *J Neurol Neurosurg Psychiatry.* 2000;68(5):589–94.
8. Myllylä VV, Sotaniemi KA, Illi A, Suominen K, Keränen T. Effect of entacapone, a COMT inhibitor, on the pharmacokinetics of levodopa and on cardiovascular responses in patients with Parkinson's disease. *Eur J Clin Pharmacol.* 1993;45(5):419–23.
9. Stocchi F, Barbato L, Nordera G, Bolner A, Caraceni T. Entacapone improves the pharmacokinetic and therapeutic response of controlled release levodopa/carbidopa in Parkinson's patients. *J Neural Transm.* 2004;111(2):173–80.
10. Paim CS, Gonçalves HML, Miron D, Sippel J, Steppe M. Stability-indication LC determination of entacapone in tablets. *Chromatographia.* 2007;65(9–10):595–9.
11. Gordin A, Kaakkola S, Teravainen H. Clinical advantages of COMT inhibition with entacapone—a review. *J Neural Transm.* 2004;111(10–11):1343–63.
12. Thomas M. Inflammation in parkinson's disease: scientific and clinical aspects. *Inflamm Park Dis Sci Clin Asp.* ISBN:3319080458. <https://doi.org/10.1007/978-3-319-08046-8>.

13. Heikkinen H, Saraheimo M, Antila S, Ottoila P, Pentikäinen PJ. Pharmacokinetics of entacapone, a peripherally acting catechol-*O*-methyltransferase inhibitor, in man. *Eur J Clin Pharmacol*. 2001;56(11):821–6.
14. Brooks DJ, Leinonen M, Kuoppamäki M, Nissinen H. Five-year efficacy and safety of levodopa/DDCI and entacapone in patients with Parkinson's disease. *J Neural Transm*. 2008;115(6):843–9.
15. Ghoneim EM, El-Desoky HS. Electrochemistry of the COMT enzyme inhibitor entacapone and its determination in pharmaceutical formulation and human blood-pharmacokinetic study. *J Electrochem Soc*. 2016;163(2):89–98.
16. Paim CS, Martins MT, Malesuik MD, Steppe M. LC determination of entacapone in tablets: in vitro dissolution studies. *J Chromatogr Sci*. 2010;48(9):755–9.
17. Savolainen J, Leppänen J, Forsberg M, Taipale H, Nevalainen T, Huuskonen J, Gynther J, Männistö PT, Jarvinen T. Synthesis and in vitro/in vivo evaluation of novel oral *N*-alkyl- and *N,N*-dialkyl-carbamate esters of entacapone. *Life Sci*. 2000;67(2):205–16.
18. Vadlamudi HC, Yalavarthi PR, Mandava Venkata BR, Thanniru J, Vandana KR, Sundaresan CR. Potential of microemulsified entacapone drug delivery systems in the management of acute Parkinson's disease. *J Acute Dis*. 2016;5(4):315–25.
19. Tailor HR, Patel VM, Solanki AS, Patel AK. Preparation and evaluation of entacapone loaded ethyl cellulose sustained release microspheres. *World J Pharm Pharm Sci*. 2017;6(10):1083–110.
20. Mohamed MA, Atty SA, Banks CE. Thermal decomposition kinetics of the antiparkinson drug 'entacapone' under isothermal and non-isothermal conditions. *J Therm Anal Calorim*. 2017;130:2359–67.
21. Sethi KD, Hauser RA, Isaacson SH, McClain T. Levodopa/carbidopa/entacapone 200/50/200 mg (Stalevo® 200) in the treatment of Parkinson's disease: a case series. *Cases J*. 2009;2(1):7134.
22. Forsberg MM, Huotari M, Savolainen J, Männistö PT. The role of physicochemical properties of entacapone and tolcapone on their efficacy during local intrastriatal administration. *Eur J Pharm Sci*. 2005;24(5):503–11.
23. Council of Europe. *European Pharmacopoeia 7.0*.
24. <https://www.drugbank.ca/drugs/DB00494>. Accessed 24 Aug 2017.
25. Savolainen J, Forsberg M, Taipale H, Männistö PT, Järvinen K, Gynther J, Jarho P, Järvinen T. Effects of aqueous solubility and dissolution characteristics on oral bioavailability of entacapone. *Drug Dev Res*. 2000;49(4):238–44.
26. Friedman HL. Kinetics of thermal degradation of char-forming plastics from thermogravimetry. Application to a phenolic plastic. *J Polym Sci*. 1965;6C:183–95.
27. Flynn JH, Wall LA. A quick, direct method for the determination of activation energy from thermogravimetric data. *Polym Lett*. 1966;4:323–8.
28. Ozawa T. A new method of analyzing thermogravimetric data. *Bull Chem Soc Jpn*. 1965;38:1881–6.
29. Sempere J, Nomen R, Serra R, Soravilla J. The NPK method: an innovative approach for kinetic analysis of data from thermal analysis and calorimetry. *Thermochim Acta*. 2002;388:407–14.
30. Serra R, Sempere J, Nomen R. A new method for the kinetic study of thermoanalytical data: the non-parametric kinetics method. *Thermochim Acta*. 1998;316:37–45.
31. Vlase T, Vlase G, Birta N, Doca N. Comparative results of kinetic data obtained with different methods for complex decomposition step. *J Therm Anal Calorim*. 2007;88:631–5.
32. Vlase G, Bolcu C, Modra D, Budiul MM, Ledeți I, Albu P, Vlase T. Thermal behavior of phthalic anhydride-based polyesters. *J Therm Anal Calorim*. 2016;126:287–92.
33. Ceban I, Blajovan R, Vlase G, Albu P, Koppandi O, Vlase T. Thermoanalytical measurements conducted on repaglinide to estimate the kinetic triplet followed by compatibility studies between the antidiabetic agent and various excipients. *J Therm Anal Calorim*. 2016;126:195–204.
34. Wall ME. Singular value decomposition and principal component analysis. In: Berrar DP, Dubitzky W, Granzow M, editors. *A practical approach to microarray data analysis*, vol. 9. Norwell: Kluwer; 2003. p. 91–109 **LANL LA-UR-02**.
35. Šestak J, Berggren G. Study of the kinetics of the mechanism of solid-state reactions at increasing temperatures. *Thermochim Acta*. 1971;3:1–12.
36. Silverstein RM, Webster FX. *Spectrometric identification of organic compounds*. 7th ed. New York: Wiley; 1998.